Q-Ball Imaging

D. S. Tuch[1], T. G. Reese[1], M. R. Wiegell[1], V. J. Wedeen[1]

[1]Athinoula A. Martinos Center for Biomedical Imaging, Charlestown, Massachusetts, United States

Synopsis — White matter fiber crossing can be resolved by q-space diffusion imaging methods or by mixture modeling of high angular resolution diffusion imaging data. However, q-space imaging requires long acquisition times, and mixture modeling, like diffusion tensor imaging, requires a model of the underlying diffusion function. Here, we present a model-independent reconstruction scheme for spherically-sampled diffusion imaging data. The reconstruction algorithm is based on the Funk-Radon transform, an extension of the Radon transform to the sphere. The technique, termed q-ball imaging, exhibits sharper diffusion peaks relative to a comparable Cartesian q-space acquisition.

Background — Magnetic resonance diffusion tensor imaging (DTI) can resolve the mean white matter fiber orientation within a voxel [1, 2]. However, a given voxel may contain a number of fiber orientations due to, for example, intravoxel fiber crossing or clusters of diverging fibers [3-8]. Such intravoxel orientational heterogeneity can be resolved with model-independent diffusion imaging approaches such as q-space imaging or diffusion spectrum imaging (DSI) [8]. However, both q-space imaging and DSI require three-dimensional Cartesian sampling and thus require significantly longer acquisition times than DTI or high angular resolution diffusion imaging (HARDI). Fiber crossing can also be resolved with mixture modeling of HARDI data, but such approaches are heavily model-dependent [5-7]. It would be desirable to have a diffusion imaging acquisition/reconstruction scheme with the model-independence of the q-space imaging methods and the efficiency of the spherical-sampling approaches. Here, we present a novel, model-independent reconstruction algorithm for inverting spherically-sampled diffusion imaging data. The technique, termed q-ball imaging (QBI) [7], is based on the Funk-Radon forward transform which we describe in the following section.

Theory — The diffusion orientation distribution function (ODF) $\psi(\mathbf{u})$ is defined at the radial projection of the Cartesian ensemble-average diffusion propagator (EAP) $P(\mathbf{r})$ [9] onto the sphere: $\psi(\mathbf{u}) = \int P(r\mathbf{u})dr$. The ODF describes the volume of spins displacing into a solid angle about the director $\mathbf{u}$. The Funk-Radon transform, also known as the spherical Radon transform, is an integral transform on the sphere. For a function $f(\mathbf{x})$ and a given direction $\mathbf{u}$ and radius r, the Funk-Radon transform G is simply the integral on the great circle (equator) $G[f(\mathbf{x})] = \int_{\mathbf{x} \perp \mathbf{u}} f(\mathbf{x})d\mathbf{x}$ around the director (pole) $\mathbf{u}$ [10, 11]. The Funk-Radon transform of the diffusion signal yields an ODF $\varphi(\mathbf{u})$ which strongly approximates the true ODF $\psi(\mathbf{u})$. Recall the Fourier relation between the diffusion signal $E(\mathbf{q})$ and the EAP: $F[E(\mathbf{q})]=P(\mathbf{r})$ where $\mathbf{q}=\gamma\delta\mathbf{g}$ is the diffusion wavevector [12]. It can be shown [7] that the Funk-Radon transform of the diffusion signal is the zeroth-order Hankel transform H of the EAP projected onto the plane containing the great circle; that is, $\varphi(\mathbf{u}) = G[E(\mathbf{q})] = H[P_{\mathbf{u}}]$ where $P_{\mathbf{u}}$ is the EAP projected onto the plane with surface normal $\mathbf{u}$. To the degree that the mass of the zeroth-order Bessel function is concentrated at the origin, the Funk-Radon transform yields an ODF which strongly approximates the true ODF, $\varphi(\mathbf{u}) \approx \psi(\mathbf{u})$ [7]. Stated more simply, for a given diffusion direction of interest $\mathbf{u}$, simply summing the diffusion signal along an equator (great circle) around $\mathbf{u}$ yields a diffusion ODF which is approximately equal to the diffusion ODF obtained by explicit computation from a Cartesian Fourier reconstruction.

Methods — MR diffusion images were obtained on a healthy volunteer on a 3T Siemens Allegra (Erlangen, Germany). The experiments consisted of a DSI acquisition and 2 QBI acquisitions. All three experiments used a twice-refocused balanced echo EPI sequence. The slice prescription for all three experiments was identical and consisted of two sagittal slices with isotropic 2.8mm resolution and a 6.72mm gap. Whole-head MPRAGE images were also acquired for anatomical reference. The sequence parameters for the DSI experiment were TR/TE/Δ/δ=800/143/66/61ms, b_{max}=1.7×10^{4}s/mm^2. 515 q-space points were sampled on a keyhole Cartesian grid with g_{max}=40mT/m and q_{max}=0.097μm^{-1}. For both q-ball experiments, the q-space sampling points were obtained from the n=492 vertices of a 7-fold tessellated icosahedron, giving an average angular distance between sampling points of 9.30±0.76°. The sequence parameters for the first QBI experiment were TR/TE/Δ/δ=800/98/44/39ms, b_{max}=4.0×10^{3}s/mm^2, g_{max}=40mT/m, q=0.057μm^{-1}, and the parameters for the second QBI experiment were TR/TE/Δ/δ=800/130/60/55ms, b_{max}=1.2×10^{4}s/mm^2, q=0.085μm^{-1}. The DSI images were reconstructed by three-dimensional Fourier transform and then radial projection using cubic spline interpolation. The QBI images were reconstructed using the Funk-Radon transform. The great circle integrals were computed using Parzen window interpolation with a Gaussian kernel [13].

Results — The low frequency QBI (q=0.057μm^{-1}) yielded diffusion ODF maps highly similar to DSI at q=0.097μm^{-1}, although with slightly sharper diffusion peaks (**Fig. 1**). The high frequency QBI (q=0.085μm^{-1}) exhibited sharper diffusion peaks than both the DSI and low-frequency QBI. The ODF maps derived from the high-frequency QBI revealed finer fiber interdigitation than was apparent on either the DSI or low-frequency QBI.

Discussion — QBI using the Funk-Radon transform provides a model-free method for reconstructing diffusion imaging data sampled on the sphere. By varying the radius of the sphere, it is possible to specify the width of the projection kernel and, in turn, control the tradeoff between signal-to-noise and angular resolution. Further, by combining multiple sampling shells it should be possible to design more optimal projection kernels than can be achieved with a single shell.

Fig. 1. Comparison of diffusion ODF maps from (a) DSI at q_{max}=0.097μm^{-1}, (b) QBI at q=0.057μm^{-1}, and (c) QBI at q=0.085μm^{-1}. ROI: crossing of the superior longitudinal fasciculus (slf), the corona radiata (cr), and the callosal striations (cc) to motor cortex.

References — [1] Basser PJ, et al. *Biophys J*. 66:259-67, 1994. [2] Pierpaoli C, et al. *Radiology*. 201:637-48, 1996. [3] Alexander AL, et al. *Magn Reson Med*. 45:770-80, 2001. [4] Frank LR. *Magn Reson Med*. 45:935-9., 2001. [5] Frank LR. *Magn Reson Med*. 47:1083-99, 2002. [6] Tuch DS, et al. *Magn Reson Med*. 48:577-82, 2002. [7] Tuch DS. *Diffusion MRI of complex tissue structure*. Doctoral Thesis. Harvard-MIT, 2002. [8] V.J. Wedeen, et al. Proc ISMRM, 8: 82, 2000. [9] Kärger J, et al. *J Magn Reson*. 51:1-7, 1983. [10] Funk P. *Math Ann*. 77:129-135, 1916. [11] Helgason S. *The Radon Transform*. Springer-Verlag, 1999. [12] Dory DG, et al. *Magn Reson Med*. 14:435-44, 1990. [13] Parzen E. *An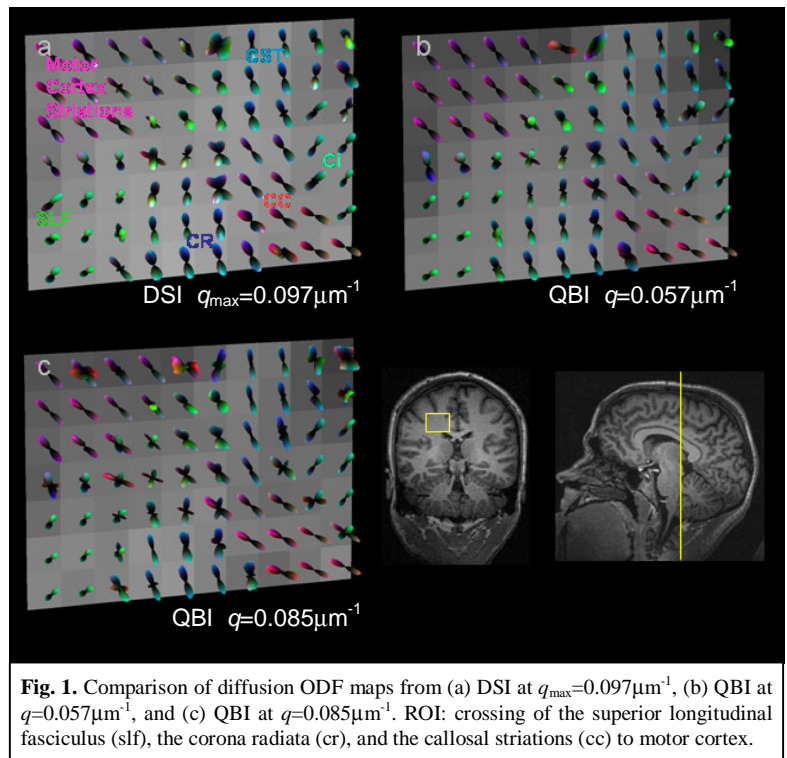n Math Stat*. 33:1065-76, 1962.